*J. Fluid Mech.* (1974), *vol.* 65, *part* 1, *pp.* 127–144
*Printed in Great Britain*



# Shock-wave structure and intermolecular collision laws

By SHEE-MANG YEN AND WINNIE NG
Coordinated Science Laboratory, University of Illinois, Urbana

(Received 26 March 1973 and in revised form 24 August 1973)

The nonlinear Boltzmann equation has been solved for shock waves in a Maxwellian gas for eight upstream Mach numbers $M_1$ ranging from 1·1 to 10. The numerical solutions were obtained by using Nordsieck's method, which was revised for use with the differential cross-section corresponding to an intermolecular force potential following an inverse fifth-power law. The accuracy of the calculations of microscopic and macroscopic properties for this collision law is comparable with that for elastic spheres published earlier (Hicks, Yen & Reilly 1972).

We have made comparisons of the detailed characteristics of the internal shock structure in a Maxwellian gas with those in a gas of elastic spheres. The purpose of this comparative study is to find the shock properties that are sensitive as well as those which are insensitive to the change in collision law and to find effective ways to study them.

The variation of thermodynamic and transport properties of interest with respect to density and to each other was found to depend only weakly on the change in collision law. The principal effect on the macroscopic shock structure due to the change in intermolecular potential is in the spatial variation of the macroscopic properties. The spatial variation of macroscopic properties may be determined accurately from the corresponding moments of the collision integral, especially in the upstream and downstream wings of the shock wave. The results for the velocity distribution function exhibit the microscopic shock characteristics influenced by a difference in intermolecular collisions, in particular the departure from equilibrium in the upstream wing of the shock and the relaxation towards equilibrium in the downstream wing. The departure of several characteristics of weak shock waves from those of the Chapman–Enskog linearized theory and the Navier–Stokes shock is also insensitive to the change in collision law. The deviation of the half-width of the function $\int f dv_y dv_z$ from the Chapman–Enskog first iterate at $M_1 = 1{\cdot}59$ is in agreement with an experiment (Muntz & Harnett 1969).

## 1. Introduction

The details of shock structure concerning the microscopic and macroscopic properties are of physical interest. Since the non-equilibrium behaviour in a shock wave is directly related to the intermolecular collisions, the shock structure changes if the intermolecular collision law changes. It would be sig-

nificant to evaluate the effect of a change of collision law on those shock properties that are of particular interest to either a theoretician or an experimentalist. For example, a physical experiment on a shock wave is often limited to the measurement of a small number of properties for selected gases. The question arises as to the way to compare the results for these properties with theoretical predictions, which are often obtained using an assumed intermolecular collision law. The difficulty in ascertaining the significance of such comparisons is twofold. First, the differential cross-sections for realistic molecular fields are difficult to determine. Second, even if the cross-sections were known, it would be extremely difficult to incorporate them in many theoretical calculations of non-equilibrium gas flows.

The use of different differential cross-sections presents no problem with Monte Carlo methods. For example, Bird has used a direct simulation technique to compute and compare density profiles in a shock wave for $M_1 = 8$ and several power laws for the intermolecular force potential (Bird 1970) and to calculate other macroscopic properties for $M_1 = 8$ and the twelfth-power law. Nordsieck's method of evaluating the collision integral in the nonlinear Boltzmann equation (Nordsieck & Hicks 1967) can also be adapted to any differential cross-section, even though this method has been applied to problems only for gases of elastic spheres, including that of the shock wave (Hicks & Yen 1969; Hicks *et al.* 1972).

In using Nordsieck's method to solve the problem of a shock wave in a gas of elastic spheres, we have computed and analysed in detail the microscopic and macroscopic characteristics of the shock-wave structure, many of which were not available before. Questions have been raised as to the deviation of these results from those for real gases which have a different intermolecular collision law. It has been our strong feeling that many of our findings are insensitive to a change in the intermolecular force potential and are thus also applicable to gases with other collision laws. This feeling is based on our belief that many of the velocity moments that determine properties of physical interest are strongly coupled.

The purpose of this paper is to show that many of our significant findings are indeed insensitive to changes in the intermolecular collision law and that the significant effects of changes in the collision law, such as in the spatial variation of properties and relaxation towards equilibrium, can accurately be determined from the collision integral, its moments and the velocity distribution itself. We have reached these conclusions by making a detailed comparison of Boltzmann solutions for a shock wave in a gas of elastic spheres with those for Maxwellian molecules (fifth-power law of intermolecular force potential) for eight upstream Mach numbers ranging from 1·1 to 10.

We shall describe briefly the method of incorporating the differential cross-section corresponding to the Maxwellian molecules, the accuracy tests and the shock solutions obtained, and then present in detail the results of our comparison of these shock-wave solutions with those for elastic spheres.

## 2. Shock-wave solutions in a Maxwellian gas

The numerical solutions of the Boltzmann equations for a shock wave in a Maxwellian gas were obtained by embedding Nordsieck's Monte Carlo method of evaluating the collision integral, revised for a Maxwellian gas, in an iterative integration scheme. The method is the same as that used to solve the Boltzmann equation for the shock wave in a gas of elastic spheres;† therefore, we need describe only the method of incorporating the differential collision cross-section of a Maxwellian gas in Nordsieck's method.

The expression for the collision integral used in Nordsieck's method is

$$a - bf = \int \frac{d\mathbf{k}}{4\pi} \int d\mathbf{v}'(FF' - ff')\,(\Omega). \tag{1}$$

We use the notation $a - bf$ for the collision integral to emphasize that the second term is proportional to $f$ and the function $b$ is positive. $F$, $F'$, $f$ and $f'$ represent the four values of the velocity distribution function corresponding to the four velocities $\mathbf{V}$, $\mathbf{V}'$, $\mathbf{v}$ and $\mathbf{v}'$. The unit vector $\mathbf{k}$ is directed along the line of centres of the molecules at the time of their closest approach. Integration is over the entire $4\pi$ solid angle in order that the $\mathbf{k}$ integration limits may be independent of $\mathbf{v}$ and $\mathbf{v}'$. The differential cross-section $\Omega$ is $|\mathbf{k}.(\mathbf{v}' - \mathbf{v})|$ for elastic spheres and a function of the deflexion angle $\chi$ for Maxwellian molecules ($\chi$ = deflexion angle of the relative velocity vector $\mathbf{v} - \mathbf{v}'$ due to collision).‡

Since the difference between the expressions for the Boltzmann integral for the two collision laws is in the differential cross-section $\Omega$, the substitution of a new collision law involves merely changing this cross-section within the computer program. In computing the collision integrals for the Maxwellian molecules, we use the Boltzmann computer program for elastic spheres§ with only one change, namely, the replacement of the differential cross-section

† Cheremisin has also developed a Monte Carlo method of evaluating the Boltzmann collision integral for a gas of elastic spheres and used it in an integral iterative scheme to solve the shock-wave and heat-transfer problems (Cheremisin 1970*a*, *b*); however, only a small number of macroscopic properties were published. Since he used the position co-ordinate as the independent variable, he did not make all the possible comparisons. However, some of his results were found to be in good agreement with ours. Chorin (1972) proposed a direct quadrature method and solved the shock-wave problem for elastic spheres for Mach numbers less than 2.

‡ The expression first given by Wang-Chang (Wang-Chang & Uhlenbeck 1952) is in error by a factor of $2^{-\frac{1}{2}}$. This error was corrected in a recent publication (de Boer & Uhlenbeck 1970, p. 70).

§ The accuracy of our computation of the Boltzmann collision integrals for a gas of elastic spheres using this computer program has been further ascertained by comparing for several Mach numbers the calculated Mott-Smith (1951) distribution functions with analytical solutions calculated using Narasimha's (Deshpande & Narasimha 1969) computer program which were for the same distribution function and gas. For this comparison, we used a large sample size (131000) for our Monte Carlo calculations to minimize the statistical error. Narasimha's computer program was revised to output the analytical calculation in the same format. Our results were found to be in good agreement for most velocity bins. The results of comparison with analytical and other calculations for elastic spheres were presented at the 7th International Rarefied Gas Dynamics Symposium, Pisa, Italy (Hicks & Yen 1973).

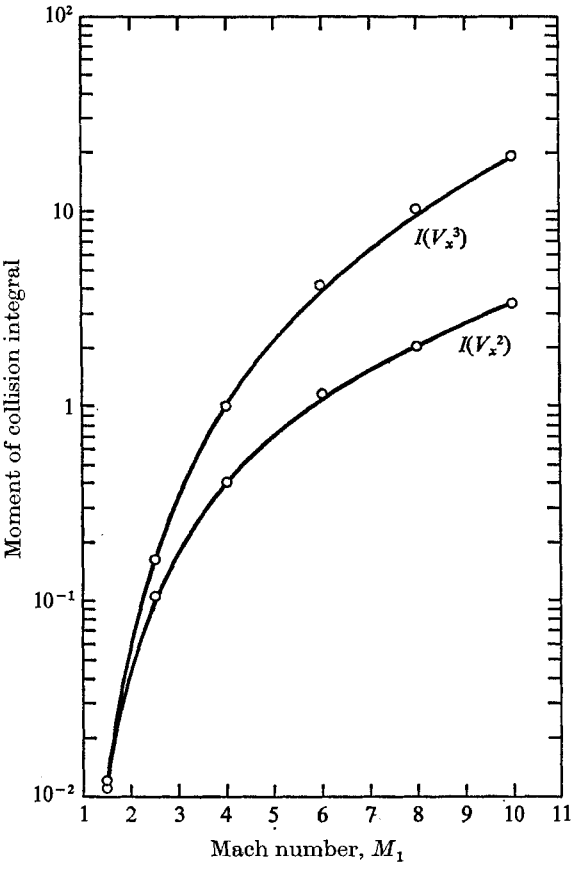


FIGURE 1. Comparison of Monte Carlo calculations of two moments of collision integral for Mott-Smith distribution function at $\hat{n} = \frac{1}{2}$, $[I_{MS}(v_x^2)]_{\hat{n}=\frac{1}{2}}$ and $[I_{MS}(v_x^3)]_{\hat{n}=\frac{1}{2}}$, for six Mach numbers. $[I_{MS}(\phi)]_{\hat{n}=\frac{1}{2}} = \int \phi[(a-bf)_{MS}]_{\hat{n}=\frac{1}{2}} d\mathbf{v}$; $\hat{n} = (n-n_1)/(n_2-n_1)$. ——, analytical calculations; ○, Monte Carlo. The average probable error of Monte Carlo calculation is less than 4 %.

$|\mathbf{k}.(\mathbf{v}'-\mathbf{v})|$ by a table of values for Maxwellian molecules. For each collision selected, the value of the differential cross-section needed is obtained from this table through interpolation.

We use $l_1/2^{\frac{1}{2}}$ as the unit of length. The mean free path $l_1$ upstream for Maxwellian molecules is defined as

$$l_1 = \frac{1}{A}\frac{1}{n_1}\left(\frac{m}{\kappa}\right)^{\frac{1}{2}}\left(\frac{kt_1}{m}\right), \tag{2}$$

where $A = 6\pi^{\frac{1}{2}}0{\cdot}499A_2(5)$ and $A_2(5) = 0{\cdot}436$. Equation (2) is based upon the following relation between the viscosity coefficient $\mu$ and the mean free path in order to be consistent with the case for elastic spheres:

$$\mu = 0{\cdot}499(nml)\,(8kt/\pi m)^{\frac{1}{2}}. \tag{3}$$

One of the tests of the accuracy the computations was to compare two moments of the collision integral for the Mott-Smith distribution function for six Mach

numbers in the range 1·5–10. As shown in figure 1, the Monte Carlo results are in excellent agreement with the analytical calculations.

The Boltzmann equation we use is of the following form:

$$v_x \partial f/\partial x = a - bf = \int (FF' - ff')\,(\Omega)\, d\mathbf{v}'(d\mathbf{k}/4\pi), \tag{4}$$

where $f = f(\mathbf{v}, x)$ is the velocity distribution function; $x$ is the distance variable in the direction perpendicular to the shock. In (4), the units we use are the values, denoted by the subscript 1, of various properties of the upstream gas. Thus $n_1$ and $t_1$ are the units of number density $n$ and temperature $t$. The unit of length $l_1 = 1/2\pi n_1 \sigma^2 = (\text{mean free path})_1/2^{\frac{1}{2}}$. The unit of velocity

$$c_1 = (2\pi k t_1 m)^{\frac{1}{2}} = (\text{mean speed})_1 \times \tfrac{1}{2}\pi.$$

The unit of time is therefore $(\text{mean free time})_1 \times (2/\pi)^{\frac{1}{2}}$ and the unit of the velocity distribution function is $n_1/c_1^3$.

Briefly, the iterative scheme to obtain the Boltzmann solution (specifically, to find the velocity distribution function at the 226 positions in velocity space at each chosen position in the shock wave) consists of the following steps.

(*a*) Assume an initial distribution function $f^0(n, \mathbf{v})$ equal to the Mott-Smith distribution function.

(*b*) Evaluate the collision integral for this $f$ at each $n$.

(*c*) Integrate the 226 Boltzmann difference equations.

(*d*) Repeat steps (*b*) and (*c*) to perform successive iterations.

Solutions were obtained for eight Mach numbers in the range $M_1 = 1{\cdot}1$–10. Nine stations dividing the variable $n$ equally and Monte Carlo samples of $2^{13}$ collisions were generally used. Four independent runs were made to obtain the statistical errors.

The accuracy of the solutions has been determined further by checking the following two relations between two moments of the collision integrals and several macroscopic properties:

$$I(v_x^2)/p\tau = t/t_1, \tag{5}$$

$$I(v_x v^2)/(-\tfrac{4}{3}pq) = t/t_1, \tag{6}$$

where $I(\phi) =$ moment of the collision integral $= \int \phi(a - bf)\, d\mathbf{v}$, $a - bf =$ collision integral, $p =$ pressure, $\tau =$ stress, $q =$ heat flux and $t =$ temperature. It was found that the relations (5) and (6) hold well for our solutions for the shock wave for Maxwellian molecules (Nathenson, Baganoff & Yen 1973).

We shall discuss in the following sections the characteristics of a shock wave in a Maxwellian gas, the comparison with those in a gas of elastic spheres and the effect of the collision law on shock properties.†

## 3. Density gradient and reciprocal shock thickness

As indicated in our paper on shock-wave structure in a gas of elastic spheres (Hicks *et al.* 1972), presenting results as density gradient $dn/dx$ *vs.* reduced density $\hat{n}$ instead of $n$ *vs.* $x$ has the advantage of showing clearly the asymmetry

† A small part of the results appear in Yen *et al.* (1973).

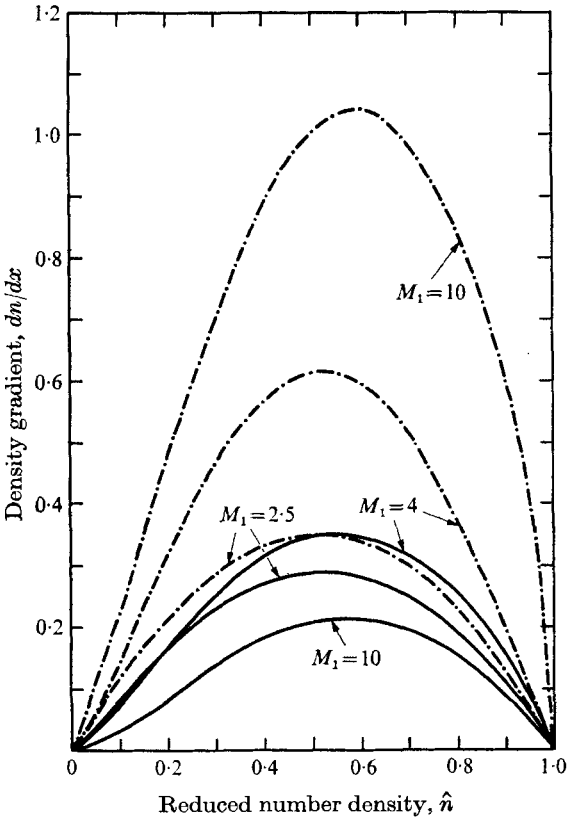


FIGURE 2. Comparison of density gradients $dn/dx$ for three values of $M_1$. ——, Maxwellian molecules; —·—·—, elastic spheres. The average probable error is 0·00931.

and the relaxation in the wings of the shock wave. Furthermore, the reciprocal shock thickness can be determined more accurately from such plots.

We compute all the gradients of the moments of the velocity distribution function and of the macroscopic properties from the related moments of the collision integrals since, for one-dimensional flow,

$$d[\mathscr{M}(\phi)]/dx = I(\phi/v_x), \tag{7}$$

where $\mathscr{M}(\phi)$ = moment of distribution function $= \int \phi f \, d\mathbf{v}$,

$I(\phi)$ = moment of collision integral $= \int \phi(a - bf)\, d\mathbf{v}$.

The moment of the collision integral $I(1/v_x)$ is thus equal to the density gradient $dn/dx$. It can be shown that the temperature and stress gradients are related to $I(v_\perp^2/v_x)$ and the heat-flux gradients to $I(v_\perp^2/v_x)$ and $I(v_x^2)$.

Figure 2 shows the density gradient $dn/dx$ *vs.* the reduced number density $\hat{n}$ for $M_1 = 2{\cdot}5$, 4 and 10. The corresponding results for elastic spheres are also shown for comparison. We observe clearly the difference in the relaxation rates and their changes with respect to $\hat{n}$ between the two shocks, especially in the wings. We shall comment further on the differences in § 5, where the gradients of

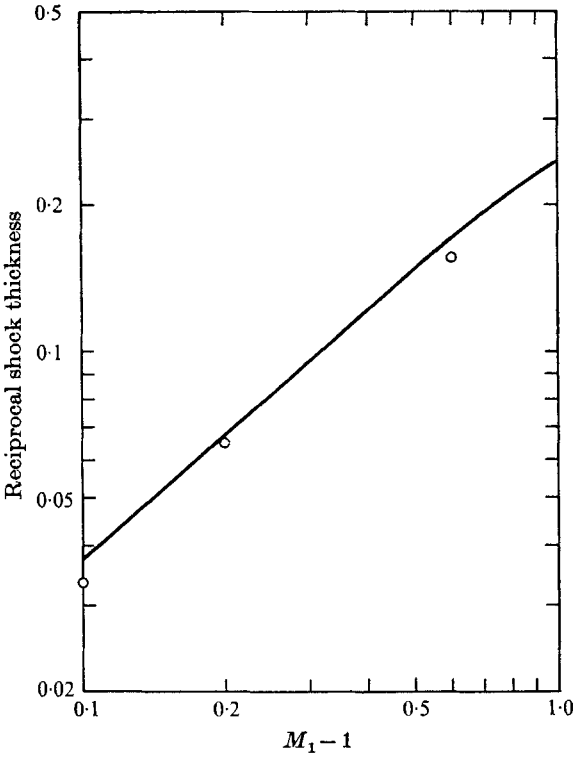


FIGURE 3. Variation of reciprocal shock thickness with Mach number $M_1$ for $M_1 < 2$. ——, Navier–Stokes; ○, Boltzmann. The probable error for the Boltzmann calculation is less than 6 %.

properties are discussed in general. The agreement of $dn/dx$ with the Navier–Stokes shock for $M_1 = 1{\cdot}2$ will be discussed in § 6, in which the characteristics of the weak shocks are compared.

We obtain from these plots of the density gradient the maximum value and calculate the reciprocal shock thickness $T_{rs}$ according to the expression

$$T_{rs} = 2\tfrac{1}{2}(dn/dx)/(n_2 - n_1). \tag{8}$$

The results for the reciprocal shock thickness are shown in figure 3 for weak shocks and in figure 4 for strong shocks. Our Boltzmann calculations are seen to be slightly lower than the Navier–Stokes values for $M_1 = 1{\cdot}1$, $1{\cdot}2$ and $1{\cdot}59$. For strong shocks, the Boltzmann calculations are in agreement with the Mott-Smith result for the $v_x v_\perp^2$ moment for $M_1 = 2{\cdot}5$, 4 and 10 and are closer to the Mott-Smith result for the $v_x^2$ moment for $M_1 = 6$ and 8. Bird's (1970) result for $M_1 = 8$ seems to be in agreement with the Mott-Smith result for the $v_x v_\perp^2$ moment.

The density profiles may be calculated by numerical integration from $d\hat{n}/dx$:

$$x(\hat{n}) = \int_{n=\hat{n}_{\max}}^{n} (dx/d\hat{n})\, d\hat{n},$$

in which $\hat{n}_{\max}$ is the reduced density at which $d\hat{n}/dx$ is maximum. We made this calculation for $M_1 = 8$ in order to make a comparison with Bird's (1970) results.

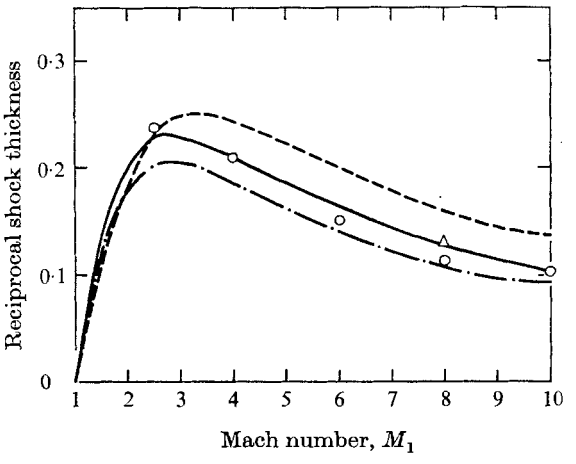


FIGURE 4. Comparison of reciprocal shock thickness as a function of $M_1$ with the Mott-Smith results. ——, Mott-Smith ($v_x v_\perp^2$); – – –, Mott-Smith ($v_x^2$); —·—, Mott-Smith ($v_x^3$); ○, Boltzmann; △, Bird. The probable error for the Boltzmann calculation is less than 3·5 %.

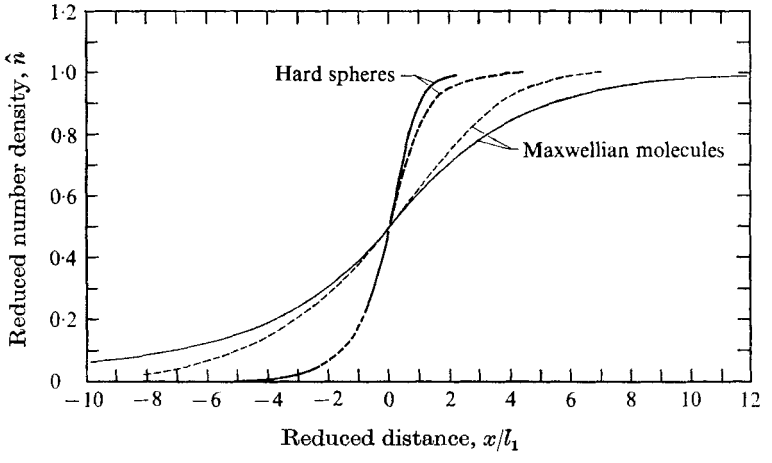


FIGURE 5. Comparison of density profiles for $M_1 = 8$. $\hat{n} = (n-n_1)/(n_2-n_1)$, $l_1$ = upstream mean free path. – – – –, Bird.

Figure 5 shows the comparison for both elastic spheres and Maxwellian molecules. Our results are in agreement with Bird's calculations for elastic spheres; however, for Maxwellian molecules, Bird's density profile seems to give a faster relaxation rate. Since our method is different from Bird's technique, it will not be possible to assess the relative systematic error in a given shock-wave property for a given collision law. (Systematic error exists in all numerical calculations.) Furthermore, for this particular calculation, our density profiles were evaluated from a moment of the collision integral, not from a moment of the distribution function, as done by Bird.

It would be significant to establish the accuracy of the calculated value of a given shock-wave property, such as the density profile, by comparing it with

an accurate experiment. A comparison was made of Bird's calculation of the density profile for the twelfth-power law for $M_1 = 8$ with an experiment for argon (Schmidt 1969), and excellent agreement was obtained.† Schmidt felt that such agreement confirmed the finding of a heat-transfer experiment that the twelfth-power collision law is suitable for argon since, according to his observation, the differences in the density profiles for the eleventh- and twelfth-power laws are significant. However, Bird (1970) has carefully studied the results and seemed to have reservations on this conclusion because of the lack of reproducibility in the heat-transfer data from which the power of the collision law was determined and the lack of discrimination of his calculation of the density profile between even the ninth- and twelfth-power laws at $M_1 = 8$.

We have also computed the asymmetry ratio $Q$ according to the following expression:‡

$$Q = \left\{\int_0^{\hat{n}_{\max}} [\hat{n}/d\hat{n}/dx]\, d\hat{n}\right\} \Big/ \left\{\int_{\hat{n}_{\max}}^1 [(1-\hat{n})/d\hat{n}/dx]\, d\hat{n}\right\}. \tag{9}$$

We found that this ratio is smaller than one for Mach numbers below about 1·5, indicating that the peak of the density profile moves from the cold side to the hot side of the shock wave as the Mach number increases. We have observed similar characteristics for the weaker shock wave for elastic spheres (Hicks *et al.* 1972).

## 4. Moments of velocity distribution function and macroscopic properties

We can calculate all the ordinary macroscopic properties of a non-equilibrium gas from six moments of the velocity distribution function $f$ (Hicks *et al.* 1972). The six moments are $n = \mathscr{M}_1$, and $\mathscr{M}_2$, $\mathscr{M}_3$, $\mathscr{M}_4$, $\mathscr{M}_6$ and $\mathscr{M}_9$, where

$$\mathscr{M}_k = \int f \Phi_k \, d\mathbf{v} \tag{10}$$

and $\Phi_1 = 1$, $\Phi_2 = v_x$, $\Phi_3 = v_x^2$, $\Phi_4 = v_x v^2$, $\Phi_6 = v_x^3$, $\Phi_9 = v_\perp^2$.

The moments $\mathscr{M}_2$, $\mathscr{M}_3$ and $\mathscr{M}_4$ are the invariants.

The reduced dimensionless properties derived from some of the six moments are

$$u = \mathscr{M}_2/n \quad \text{(gas velocity)}, \tag{11}$$

$$t_x = 2\pi[-u^2 + \mathscr{M}_3/n] \quad \text{(longitudinal temperature)}, \tag{12}$$

$$t_\perp = \pi \mathscr{M}_9/n \quad \text{(lateral temperature)}, \tag{13}$$

$$t = \tfrac{1}{3}t_x + \tfrac{2}{3}t_\perp \quad \text{(temperature)}, \tag{14}$$

$$\tau = \tfrac{2}{3}n(t_\perp - t_x) \quad \text{(stress)}, \tag{15}$$

$$q = (2\pi \mathscr{M}_4/\mathscr{M}_2) - 3t_x - 2t_\perp - 2\pi u^2 \quad \text{(total heat flux)}, \tag{16}$$

$$q_x = (2\pi \mathscr{M}_6/\mathscr{M}_2) - 3t_x - 2\pi u^2 \quad \text{(longitudinal heat flux)}. \tag{17}$$

† Since the difference in the density profile between the gas of elastic spheres and that of twelfth-power law was found to be small (Bird 1970), we may expect that our result on this property if calculated according to the twelfth-power law would also be in agreement with Schmidt's experiment.

‡ First used by Schmidt (1969).

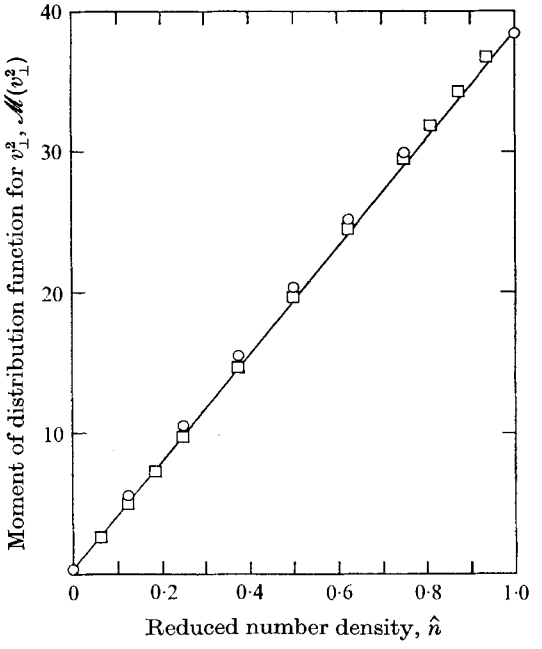


FIGURE 6. Variation of moment $\mathscr{M}(v_\perp^2) = \int v_\perp^2 f \mathrm{d}\mathbf{v}$ of distribution function as a function of reduced number density $\hat{n} = (n-n_1)/(n_2-n_1)$ for $M_1 = 10$. ○, Maxwellian molecules; □, elastic spheres. Maximum probable error is less than 2 %.

In accordance with our definition of units above, the units of the dimensional quantities (corresponding to the dimensionless quantities $u$, $t$, $\tau$ and $q$) are, respectively, $u_1$, $t_1$, $p_1$ and $u_1^2$.

Our calculations show that each of five non-invariant moments of $f$ ($\mathscr{M}_4$, $\mathscr{M}_6$, $\mathscr{M}_9$ and two other moments) is nearly a linear function of the density $n$. One of these results is shown in figure 6, in which $\mathscr{M}_9$ is plotted *vs.* $\hat{n}$ for $M_1 = 10$. As shown in this figure, the shock wave for the case of elastic spheres also exhibits the linearity (Hicks *et al.* 1972). We thus observe that the moments of $f$ that determine the ordinary macroscopic properties are strongly coupled and that this coupling depends very weakly on the intermolecular collision law. We might, therefore, expect that the variation of macroscopic properties with respect to $n$ and to each other would be nearly the same for a gas whose intermolecular collision law lay between the two extreme cases of elastic spheres and Maxwellian molecules. It should be noted that the Mott-Smith shock predicts an exactly linear dependence of the moments of $f$ on $n$ and, therefore, independence of the collision law for the variation of macroscopic properties with respect to $n$.

The variation of the heat fluxes and the stress with respect to $\hat{n}$ is shown in figure 7 for $M_1 = 4$ for three shocks: the Boltzmann shock in a Maxwellian gas, the Boltzmann shock for elastic spheres and the Mott-Smith shock. The overall variation of each of the three properties among the three shocks is seen to be very close; however, the differences are significant, especially in the upstream and the downstream wings.

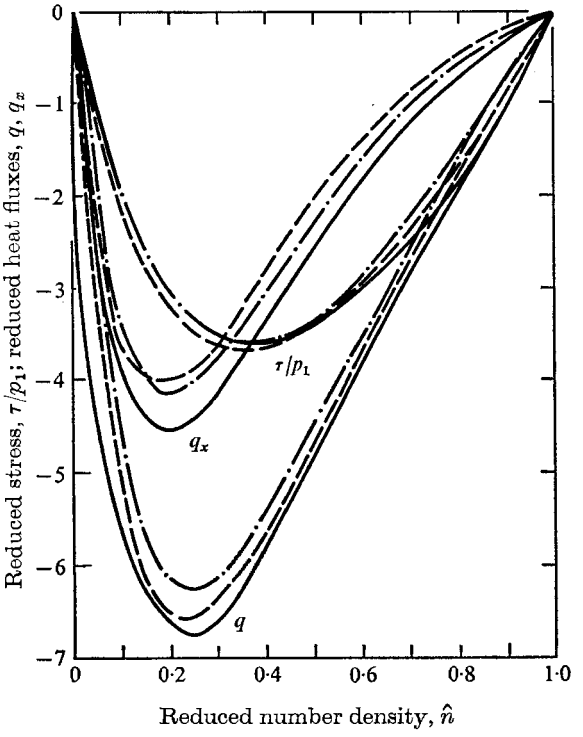


FIGURE 7. Comparison of variation of stress $\tau/p_1$, heat flux $q$ and heat flux $q_x$ associated with longitudinal motion with reduced density $\hat{n}$ for $\mathscr{M}_1 = 4$. ——, Boltzmann–Maxwellian molecules; —·—, Boltzmann–elastic spheres; – – –, Mott-Smith. Average probable errors for the Boltzmann calculations are less than 0·06 for $\tau/p_1$ and $q_x$ and less than 0·12 for $q$.

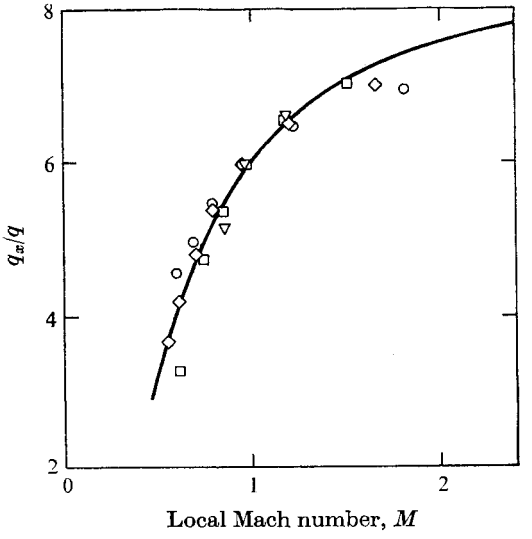


FIGURE 8. Variation of heat flux ratio $q_x/q$ with local Mach number $M$ for different values of $M_1$. ——, theory of Baganoff & Nathenson. Boltzmann–Maxwellian molecules: ▽, $M_1 = 1{\cdot}2$; □, $M_1 = 2{\cdot}5$; ◇, $M_1 = 4$; ○, $M_1 = 10$.

For the shock structure in a gas of elastic spheres, we have discussed other moments and properties as functions of density (Hicks *et al.* 1972). These functions would also be insensitive to a change in collision law. We show in figure 8 the ratio $q_x/q$ as an example. It was found also to correlate well with the local Mach number according to a model predicted by Baganoff & Nathenson (1970).

## 5. Spatial gradients of shock properties

In § 4 we discussed the strong coupling among macroscopic shock properties and its relative insensitivity to changes in the intermolecular collision law. We shall turn our attention here to the spatial gradient of macroscopic properties, which strongly depends on the intermolecular collision law. As indicated in § 3, we study such gradients on the basis of our calculations of the moments of the collision integral [see equation (7)].

We have studied three moments of the collision integral: $I(1/v_x)$, $I(v_\perp^2/v_x)$ and $I(v_x^2)$. The density gradient is determined by $I(1/v_x)$. The temperature and stress gradients are related to $I(v_\perp^2/v_x)$, and the heat flux gradients to $I(v_\perp^2/v_x)$ and $I(v_x^2)$.

The moment $I(1/v_x)$ for shocks for both elastic spheres and Maxwellian molecules, plotted for several Mach numbers in figure 3, is discussed in § 3. The moments $I(v_x^2)$ and $I(v_\perp^2/v_x)$ for $M_1 = 10$ are shown in figures 9(*a*) and (*b*) respectively. The difference in the relaxation rates for these two moments for the two shocks is qualitatively similar to that for $I(1/v_x)$.

In order to make a quantitative assessment of the differences in the moments of the collision integrals and the corresponding gradients in moments of the distribution function, we show in table 1 the ratio of the three moments $[I(\phi)]_{MM}$ for Maxwellian molecules and $[I(\phi)]_{ES}$ for elastic spheres at several positions in a shock wave for $M_1 = 4$ and 10. We observe that the ratio is nearly constant in the range of $\hat{n} = \frac{1}{4} - \frac{5}{8}$ but that it is different in the upstream ($\hat{n} = \frac{1}{8}$) or downstream ($\hat{n} = \frac{3}{4}, \frac{7}{8}$) wings. It seems, therefore, that there are three distinct regions in which the effects of the intermolecular potentials differ. We also see that the variation of these ratios with respect to density $\hat{n}$ for all three moments is nearly the same for the two Mach numbers. This also implies that the variation of one property with respect to the others is also nearly the same and, thus, its dependency on the collision law is slight. (This conclusion is of course consistent with the same finding based on the fact that several moments of the distribution function in a shock wave are almost linear functions of the density for both gases.)

We thus see that the principal effect of the intermolecular collision law for soft molecules on macroscopic properties is in the magnitude of their relaxation rates and, in addition, the nature of the relaxation in the upstream and downstream wings. Since the nature of the relaxation in the interior of the shock is similar for three moments of physical interest, we are able to justify those theoretical and experimental studies of the effect of intermolecular collisions which look at only the density gradients by the following statement. Except in the upstream and downstream wings, the spatial variation of shock properties can be determined fairly well from that of any property, e.g. $n(x)$, which can be obtained more easily in most experimental and theoretical studies.

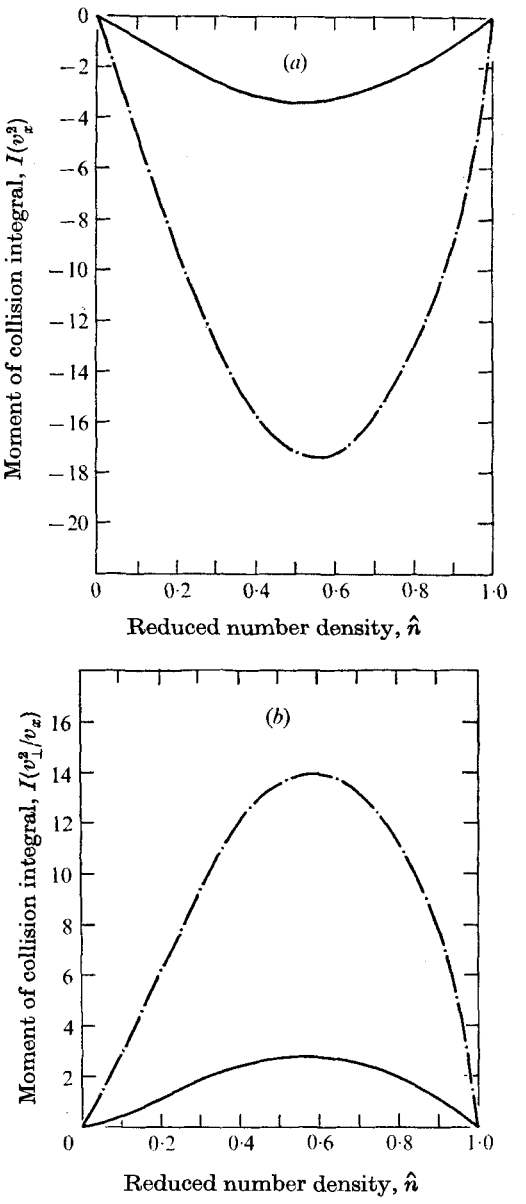


FIGURE 9. Comparison of variation of moments of (*a*) $I(v_x^2)$ and (*b*) $I(v_\perp^2/v_x)$ of collision integral with $\hat{n}$ for $M_1 = 10$. ——, Maxwellian molecules; —·—, elastic spheres. Average probable error is less than 6 %.

## 6. Comparison with Navier–Stokes shock at a low Mach number ($M_1 = 1{\cdot}2$)

In the comparison with the Navier–Stokes shock in a gas of elastic spheres (Hicks *et al.* 1972), we have found that (i) the Boltzmann density gradient is lower than the corresponding Navier–Stokes value for $\hat{n} > 0{\cdot}2$, (ii) the $dt/dn$ *vs.* $\hat{n}$ profiles are in agreement, (iii) the value of the Prandtl number $Pr$ is nearly

| $n$ \ $\phi$ | $M_1 = 4$ | | | $M_1 = 10$ | | |
|---|---|---|---|---|---|---|
| | $1/v_x$ | $v_\perp^2/v_x$ | $v_x^2$ | $1/v_x$ | $v_\perp^2/v_x$ | $v_x^2$ |
| $\frac{1}{8}$ | 0·52 | 0·53 | 0·61 | 0·15 | 0·16 | 0·19 |
| $\frac{1}{4}$ | 0·55 | 0·54 | 0·56 | 0·19 | 0·20 | 0·19 |
| $\frac{3}{8}$ | 0·55 | 0·53 | 0·55 | 0·20 | 0·20 | 0·20 |
| $\frac{1}{2}$ | 0·57 | 0·55 | 0·54 | 0·21 | 0·20 | 0·20 |
| $\frac{5}{8}$ | 0·58 | 0·55 | 0·55 | 0·20 | 0·19 | 0·19 |
| $\frac{3}{4}$ | 0·63 | 0·62 | 0·58 | 0·19 | 0·19 | 0·17 |
| $\frac{7}{8}$ | 0·75 | 0·71 | 0·69 | 0·18 | 0·15 | 0·14 |

TABLE 1. Ratio $[I(\phi)]_{MM}/[I(\phi)]_{ES}$ of collision integrals. (Average probable errors for $I(\phi)$ less than 6 %.)

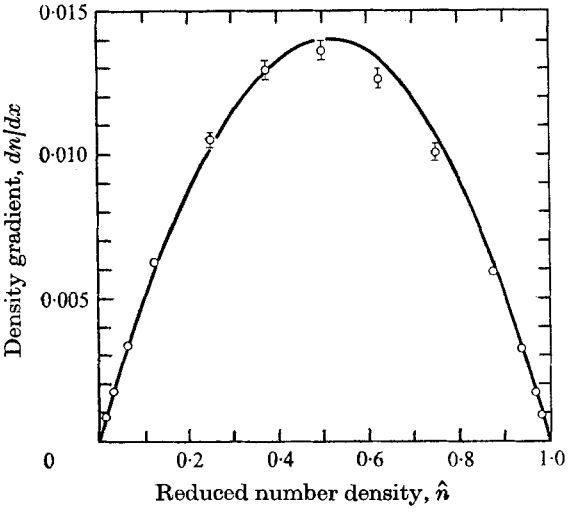


FIGURE 10. Comparison of density gradient $dn/dx$ for Boltzmann–Maxwellian molecules with Navier–Stokes results for $M_1 = 1{\cdot}2$. ——, Navier–Stokes; $\bar{\varphi}$, Boltzmann–Maxwellian molecules, indicating probable error.

constant in the interior of the Boltzmann shock and (iv) the viscosity–temperature relation in the Boltzmann shock departs considerably from that of the linearized theory especially in the downstream half of the shock. We have made the same comparative study and shall discuss the results here

As shown in figure 10, the Boltzmann density gradient for Maxwellian molecules is in good agreement with the Navier–Stokes shock corresponding to the viscosity–temperature relation $\mu/\mu_1 = t/t_1$. As indicated above, the density gradient, except in the upstream wing, is lower than the Navier–Stokes results for the case of elastic spheres.

Our findings on the variation of $dt/dn$, $Pr$ and the viscosity–temperature relation with respect to reduced density $\hat{n}$ are essentially the same as those for

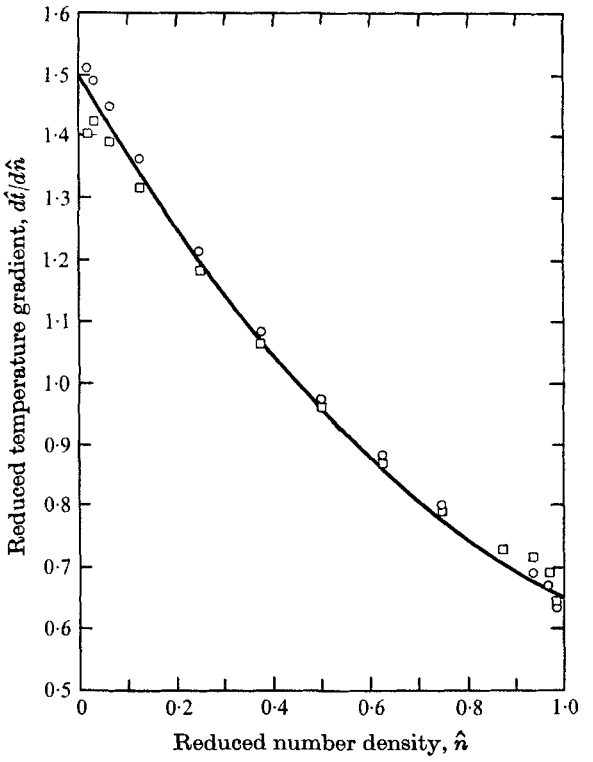


FIGURE 11. Comparison of Boltzmann gradient $d\hat{t}/d\hat{n}$ of reduced temperature with the Navier–Stokes values for $M_1 = 1{\cdot}2$. ——, Navier–Stokes; ○, Boltzmann–Maxwellian molecules; □, Boltzmann–elastic spheres. Average probable error for the Boltzmann calculations is less than 0·0065.

the elastic spheres. We compare these results in figures 11, 12 and 13. It should be pointed out that we use

$$\mu_{\text{rel}} = \begin{cases} (\mu/\mu_1)/(t/t_1)^{\frac{1}{2}} & \text{for elastic spheres,} \\ (\mu/\mu_1)/(t/t_1) & \text{for Maxwellian molecules.} \end{cases}$$

For a Chapman–Enskog gas (i.e. for small values of $M_1 - 1$), $\mu_{\text{rel}}$ should be equal to one.

## 7. Velocity distribution function

We have monitored the difference between the velocity distribution functions of the two Boltzmann shocks for $M_1 = 4$ through our computer graphical display system. (The layout of the velocity space for the direct display of the velocity-dependent functions is shown in figure 14.) We shall discuss the qualitative features of the difference in the distribution functions for the two shocks for this Mach number, as exhibited by the graphical display.

Representative distribution functions $f$ at five positions

$$(\hat{n} = (n - n_1)/(n_2 - n_1) = \tfrac{1}{8}, \tfrac{1}{4}, \tfrac{1}{2}, \tfrac{3}{4} \text{ and } \tfrac{7}{8})$$

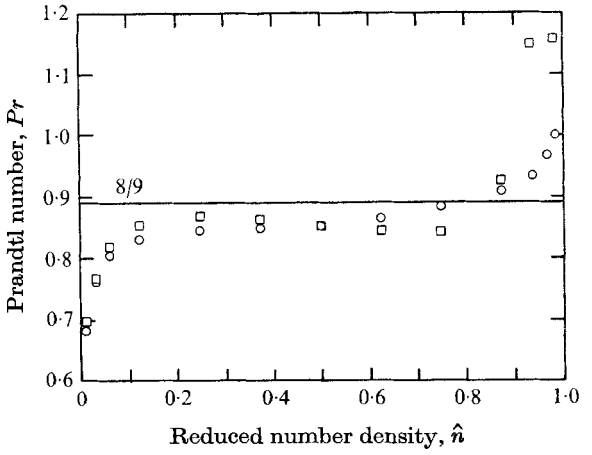


FIGURE 12. Variation of Prandtl number $Pr$ with reduced density $\hat{n}$ for $M_1 = 1{\cdot}2$. ○, Boltzmann–Maxwellian molecules; □, Boltzmann–elastic spheres. Average probable error < 0·03.

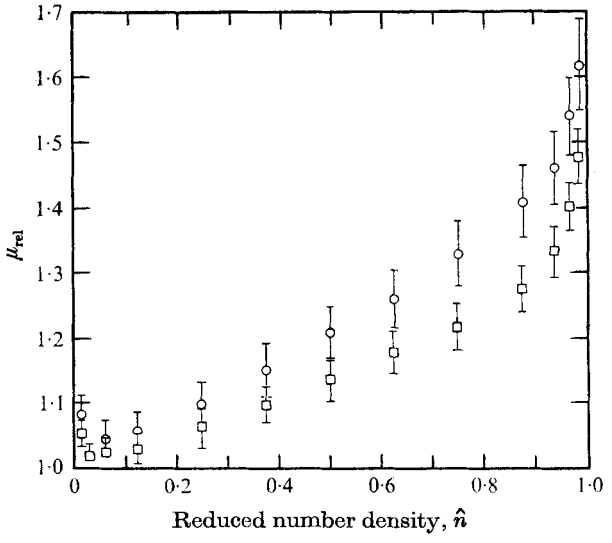


FIGURE 13. Variation of the viscosity–temperature ratio $\mu_{\text{rel}}$. $\mu_{\text{rel}} = (\mu/\mu_1)/(t/t_1)$ for Maxwellian molecules. $\mu_{\text{rel}} = (\mu/\mu_1)/(t/t_1)^{\frac{1}{2}}$ for elastic spheres. ⊕, Boltzmann–Maxwellian molecules, showing probable error; ⊞, Boltzmann–elastic spheres, showing probable error.

are shown in figures 15 (*a*) and (*b*) (plates 1 and 2) for both Maxwellian molecules and elastic spheres. (The scale for each display is different and is adjusted to have the same maximum height for each figure to show the detailed feature.) These pictures show clearly the following three differences: (i) the deep penetration of high speed molecules from the cold side towards the hot side in the case of elastic spheres (indicated by the sharp peaks on the positive-$v_x$ side throughout the shock) and the lack of it for the Maxwellian molecules, (ii) that the bimodal characteristics of the distribution functions are less pronounced in the case of

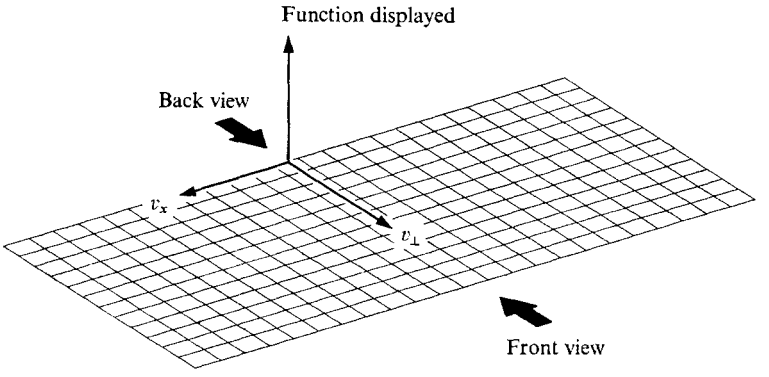


FIGURE 14. Computer graphical display.

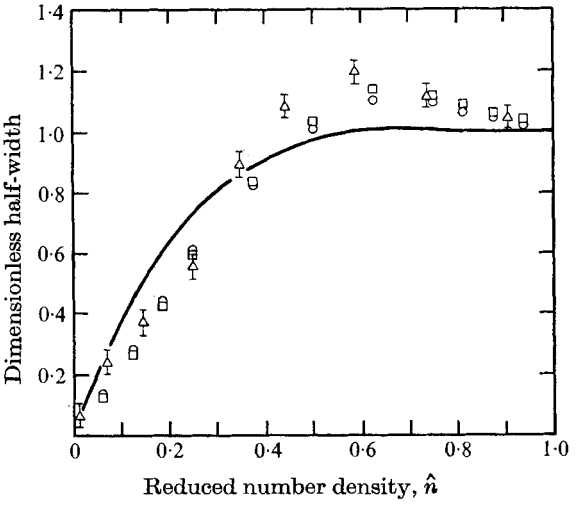


FIGURE 16. Comparison with an experiment of the Boltzmann results for the half-width $\overline{W} = (W - W_1)/(W_2 - W_1)$ of the distribution function $f(v_x) = \int f dv_y dv_z$ in a shock wave at $M_1 = 1{\cdot}59$. ——, Chapman–Enskog; ⧖, experiment (helium), Muntz & Harnett; ○, Boltzmann–Maxwellian molecules; □, Boltzmann–elastic spheres. Maximum probable error for the Boltzmann calculations is less than 1 %.

Maxwellian molecules, and (iii) that the relaxation towards equilibrium in the downstream wing is completed earlier for Maxwellian molecules (indicated by the observation that, for Maxwellian molecules, the distribution functions at $\hat{n} = \frac{3}{4}$ and $\frac{7}{8}$ are much closer to the equilibrium values than the corresponding distribution functions for elastic spheres).

Muntz & Harnett (1969) have made two experimental measurements of certain distribution functions for $M_1 = 1{\cdot}59$:

$$F(v_x) = \int f dv_y dv_z, \quad F(v_y) = \int f dv_x dv_z.$$

They found significant deviations of $F(v_x)$ from that of the corresponding Chapman–Enskog first iterate. The results for the half-width of $F(v_x)$ are in good agreement with our Boltzmann calculations for elastic spheres for this

Mach number (Holtz, Muntz & Yen 1971). We have made this calculation also for Maxwellian molecules and, as shown in figure 16, have found the same departure from the Chapman–Enskog result. The values of the half-width for Maxwellian molecules are slightly higher than the corresponding results for elastic spheres for $\hat{n} = 0$–$\frac{1}{4}$ and slightly lower in the remaining range; however, the maximum difference between the two cases is less than 7%. It seems, therefore, that this property of the distribution function is also insensitive to the change in intermolecular collision law. This insensitivity adds significance not only to the comparative study (Holtz *et al.* 1971) but also to the experimental results of Muntz & Harnett (1969).

This work was supported in part by the Joint Services Electronics Program (U.S. Army, U.S. Navy and U.S. Air Force) under Contract DAAB-07-72-C-0259, in part by the National Oceanic and Atmospheric Administration under Grant N22-1-72-(G) and in part by the Office of Naval Research under Contract N00014-67-A-0305-0001.

## REFERENCES

BAGANOFF, D. & NATHENSON, M. 1970 *Phys. Fluids*, **13**, 596.

BIRD, G. A. 1970 *Phys. Fluids*, **13**, 1172.

BOER, J. DE & UHLENBECK, G. E. 1970 *Studies in Statistical Mechanics*, vol. 5. North-Holland.

CHEREMISIN, F. G. 1970*a* *Zh. Vych. Mat. i Mat. fiz* (*J. Comp. Math. & Math. Phys.*) **10**, 654.

CHEREMISIN, F. G. 1970*b* *Izv. Akad. Nauk SSSR, Mekh. Zhid. Gaza* (*Bull. Acad. Sci. USSR, Mech. Liquids & Gases*) **5**, 185.

CHORIN, A. J. 1972 *Comm. Pure Appl. Math.* **25**, 171.

DESHPANDE, S. M. & NARASIMHA, R. 1969 *J. Fluid Mech.* **36**, 545.

HICKS, B. L. & YEN, S. M. 1969 *Proc. 6th Int. Symp. on Rarified Gas Dynamics*, **1**, 313.

HICKS, B. L., YEN, S. M. & REILLY, B. J. 1972 *J. Fluid Mech.* **53**, 85.

HICKS, B. L. & YEN, S. M. 1973 *Proc. 7th Int. Symp. on Rarefied Gas Dynamics* (to be published).

HOLTZ, T., MUNTZ, E. P. & YEN, S. M. 1971 *Phys. Fluids*, **14**, 545.

MOTT-SMITH, H. M. 1951 *Phys. Rev.* **82**, 885.

MUNTZ, E. P. & HARNETT, L. N. 1969 *Phys. Fluids*, **12**, 2027.

NATHENSON, M., BAGANOFF, D. & YEN, S. M. 1973 *Proc. 8th Int. Symp. on Rarefied Gas Dynamic* (to be published).

NORDSIECK, A. & HICKS, B. L. 1967 *Proc. 5th Int. Symp. on Rarefied Gas Dynamics*, **1**, 675.

SCHMIDT, B. 1969 *J. Fluid Mech.* **39**, 361.

WANG-CHANG, C. S. & UHLENBECK, G. E. 1952 *University of Michigan Rep.* project M999.

YEN, S. M., WALTERS, W. P., NG, W. & FLOOD, J. R. 1973 *Proc. 8th Int. Symp. on Rarefied Gas Dynamics* (to be published).

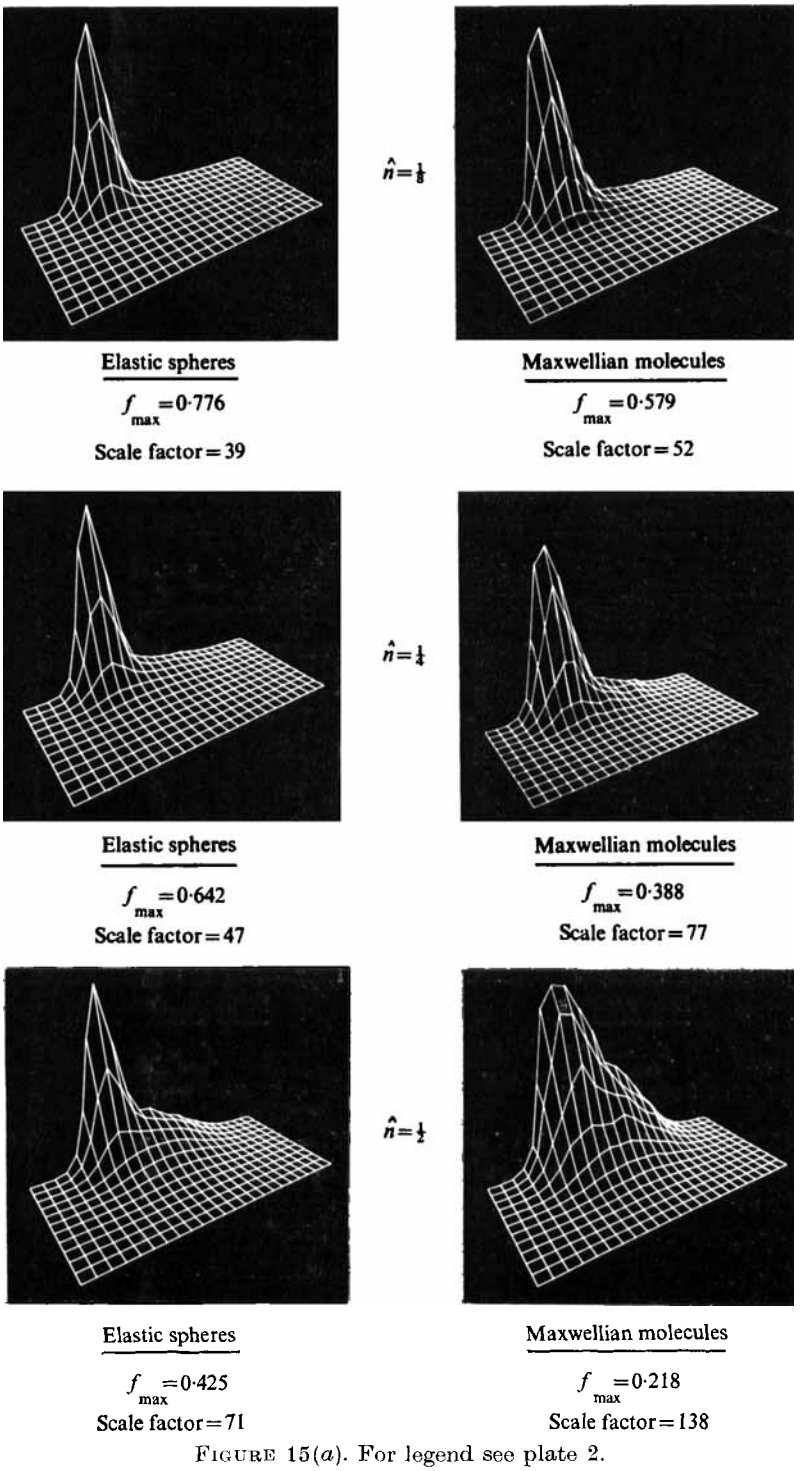


FIGURE 15(*a*). For legend see plate 2.

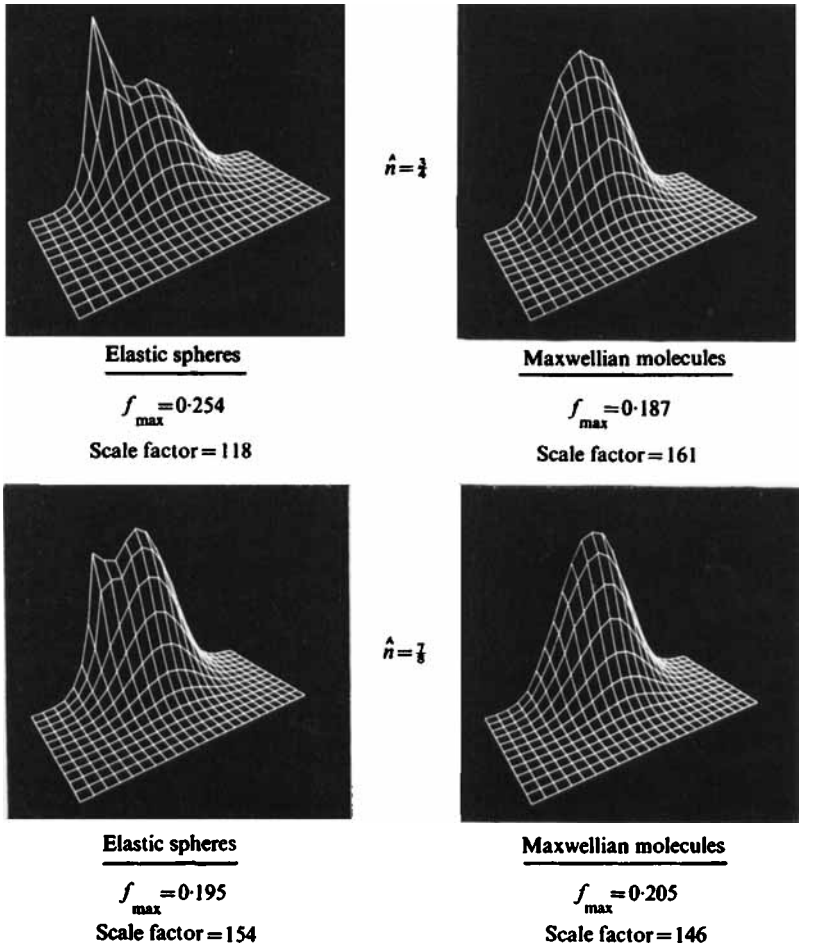


FIGURE 15. Display of distribution function $f$ for $M_1 = 4$ at various positions. (*a*) $\hat{n} = \frac{1}{8}$, $\frac{1}{4}$ and $\frac{1}{2}$. (*b*) $\hat{n} = \frac{3}{4}$ and $\frac{7}{8}$. The distribution function in arbitrary units = vertical height in figure/scale factor.